INVARIANT IMAGE DESCRIPTION FOR THE IMPROVEMENT OF MEDICAL DIAGNOSTICS

JOACHIM H. NAGEL
Department of Biomedical Engineering and Behavioral
Medicine Research Center, University of Miami

ABSTRACT

Medical imaging has become a very important diagnostic tool permitting the non-invasive assessment and presentation of anatomy, pathology, motion, blood flow, and even metabolic functions. In most cases, the images are visually inspected by experts for the diagnosis of abnormalities. The workload for these experts may be eased and their diagnostic abilities may be improved by the use of quantitative image processing techniques which have become feasible with the availability of powerful and low-cost computers. Major problems for computerized image processing, especially in multimodality imaging applications, are the combination of complementary data contained in images obtained from the same patient but at different times or with different modalities, and the determination of spatial, anatomical references, especially in cases where the image resolution is not sufficient to visually establish unequivocal correspondences between image structures and the anatomical situation. A solution to these problems can be found by introducing an invariant image description which eliminates sytem-specific parameters such as the position of an object within the image, image scale and orientation. Once the images have been transformed into such a threefold invariant representation, image contents can easily be compared and patterns are more readily detected and spatially allocated regardless of their origin and character. An algorithm for invariant image description has been developed and successfully tested in a variety of clinical applications. Results are shown for renal studies, fundus imaging, diagnosis of Alzheimer's disease, quantification of aortic stenosis, and the determination of stroke volume using ultrafast CT imaging.

Biomed Eng Appl Basis Comm, 1994 (Oct); 6: 717-728
Keyworkds: Image Processing, Image Registration, Invariant Image Descriptors, Log-Log Transform, Log-Polar Transform

INTRODUCTION

Modern medical imaging systems permit the precise and detailed presentation of anatomy, pathology, motion, flow, and even metabolic functions. Imaging by means of X-rays, magnetic resonance and ultrasound, endoscopy and photography primarily yield anatomic information, including the presentation of motion and blood flow.

Imaging techniques in nuclear medicine, such as gamma camera, single photon emission tomography and

Arrived: Aug. 26, 1994; accepted: Sept. 25, 1994
Correspondence to: Joachim H. Nagel, D.Sc.
Department of Biomedical Engineering, University of Miami, P.O. Box 248294, Coral Gables, Florida 33124, USA

positron emission tomography are used to visualize meta-bolic functions. Transitions between the different imaging techniques are gradual. Several of the mentioned modalities, primarily used to obtain information in one area, can also be used in a modified version to gain complementary information. Magnetic resonance imaging, for example, is not only suitable to show the anatomy of the patient, but can also be used for tissue characterization if, instead of proton density, the relaxation times are emphasized in the images. Furthermore, blood flow can be measured and even metabolic processes can be assessed by utilizing chemical shift imaging.

Supporting the physician in achieving the best possible evaluation of the multitude of images available, and thus contributing to the improvement of clinical diagnostics and therapy by developing the necessary technical tools and techniques, is an extraordinarily important task of Biomedical Engineering. Of special importance is the integration of different image contents. Combining the information of different images of the same patient, acquired either by different modalities or using the same technique but at different times, can often decisively improve the diagnostic possibilities.

Unfortunately, comparing or combining the information content of individual images is often associated with considerable difficulties because, as a necessary prerequisite, the pictures have to be precisely aligned and scaled, i.e. registered. The question is how to achieve a reliable and exact image registration. Functional images often exhibit very low resolution, and anatomically characteristic points, so-called landmarks, which would make the proceeding much easier, are hardly recognizable. In addition, images acquired on the basis of different physical principals or with different imaging procedures represent different parameters. Anatomic boundaries do not always match exactly the regions of metabolic activity. Differences in image scales, viewing angles, as well as the fact that in most cases images are taken at different times, result in additional problems.

In nuclear medicine images like PET scans, the resolution, as compared to NMR images, very often is not sufficient to unequivocally assign certain image structures to anatomic features. By superimposing the PET and NMR images, a spatial anatomic reference can be brought into the PET scan, whereupon sources of abnormal metabolic activity, e.g. tumors, can be assigned or localized better than with a PET scan alone.

Even with pictures like the fundus images shown in figure 1, taken with the same camera but at different times in order to detect possible anatomical changes, it is often difficult to achieve exact matching. This applies even more since it is not known à priori whether the obvious distinctions between the images are due to differences in the image acquisition, e.g. different viewing angles, or whether they appear as a result of physiological, anatomical or pathological changes of the fundus.

Clinical experience has shown that image registration, i.e. the process to align images with respect to their position, orientation and scale, poses a very complicated problem to a human expert. A reliable technique for automatic image registration therefore represents a significant help for the improvement of medical diagnostics.

IMAGE REGISTRATION

Image registration can be formally defined as the transformation of an image with regard to another image such that the characteristics of each area or volume element of the depicted object can be addressed by the

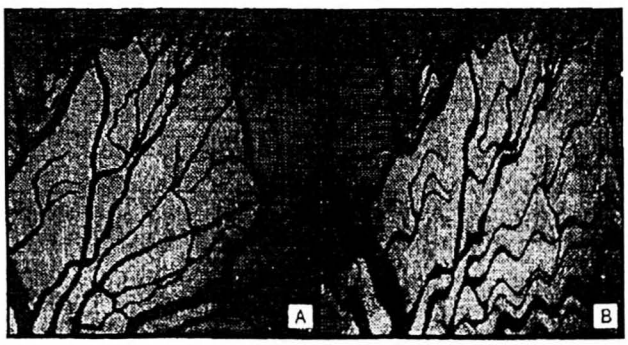

Fig. 1. Two fundus images showing the same region of the retina, but taken at different times. Image B exhibits distinct deformations compared to image A.

same coordinates in both images. That means that for any body element randomly chosen in one of the images, the matching information from the second image is immediately available.

Image registration techniques fall essentially into two categories: local and global methods. Local methods are based on the correspondence between small subgroups of imaging points, the landmarks or control points. With few exceptions, medical images are less suitable for the local methods of image registration, because a simple and reliable determination of landmarks is impossible in most cases.

Global registration techniques try to establish a single transformation for the whole image to achieve optimum registration. The dimension m of the problem corresponds to the number of possible deformation parameters. A measure of similarity is defined that represents a function of the image contents and the m-parametric transformation. The solution is the point within the m-dimensional space which achieves the highest similarity between both images. Conventional methods determine the registration parameters by exhausting search, i.e. a measure of similarity is calculated for each possible translation, rotation and scaling, and then its maximum is determined. The computational amount required for this search is enormous. Therefore, the so-called hierarchical or coarse to fine strategies have been adopted, which initially determine the approximate area of the maximum with a coarse mesh and then do a complete search in the immediate area using a fine mesh.

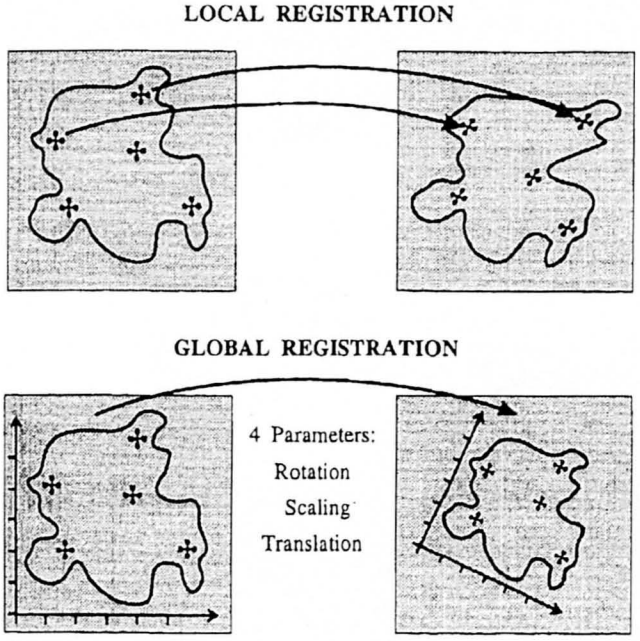

Fig. 2. Local and global image registration. Local registration is based on the matching of landmarks, requiring rubber-sheet transformations, whereas global registration determines one transformation for the whole image to achieve optimum matching.

The cross correlation function (CCF) has proven to be the most effective measure of similarity for image registration. Unlike other techniques it does not require any prior segmentation or pattern recognition, it is largely indifferent against noise, and furthermore, it utilizes the complete image information to determine the similarity.

The cross correlation function of two images $I_1(x,y)$ and $I_2(x,y)$ with their corresponding spectral representations $F_1(u,v)$ and $F_2(u,v)$, which are determined by Fourier transforms, is determined as:

$$CCF_{1,2}(x,y) = FFT^{-1} \{ F_1(u,v) \cdot F_2^*(u,v) \} \qquad (1)$$

The coordinates of the maxima, indicating the alignment with the highest similarity, determine the translation parameters for the image registration.

INVARIANT IMAGE DESCRIPTION

In a normal presentation of image information as the 2- or 3-dimensional distribution of image parameters like density, absorption coefficient etc., translation cannot be determined independent of the rotation and image scale. A substantial facilitation and simplification of image registration can be achieved by decoupling the single registration parameters, i.e. by a transformation of the image into a presentation that is invariant with regard to translation, rotation and scaling. With such an invariant image representation, the registration parame-

ters can be determined independently and one after the other, a procedure which leads to a drastic reduction of the computational amount required.

In order to demonstrate the characteristics of the threefold invariant image description, consider two pictures f(x,y) and f'(x,y) where f'(x,y) is determined by a 4-parametric geometric transformation of f(x,y):

$$f'(x,y) = f(\alpha(x\cos\beta+y\sin\beta)-\Delta x,\ \alpha(-x\sin\beta+y\cos\beta)-\Delta y) \quad (2)$$

Δx and Δy are translations, α is a uniform scaling factor and β is the angle of rotation.

Decoupling the registration parameters for translations can be achieved by utilizing the characteristics of the Fourier transform. An image shift in the spatial domain corresponds to a phase shift in the spatial frequency domain, i.e. calculating the magnitude of the Fourier spectra or the power spectra of the images eliminates the translation parameters. Thus, the images are invariant with regard to an image translation, but still contain the rotation and scaling parameters:

$$|F'(u,v)| = \frac{1}{\alpha^2}\left| F\left(\frac{(u\cos\beta+v\cos\beta)}{\alpha}, \frac{(-u\sin\beta+v\cos\beta)}{\alpha}\right)\right| \quad (3)$$

Transformation of the magnitude spectra into polar coordinates (r,θ) causes the decoupling of rotation and scaling:

$$|F'(r,\Theta)| = \frac{1}{\alpha^2}\left| F\left(\frac{r}{\alpha}, \Theta+\beta\right)\right| \quad (4)$$

$$with\ r = \sqrt{x^2+y^2}\ \ and\ \ \Theta=\tan^{-1}(y/x)$$

Rotation now appears as a cyclic shift in the angular coordinate and scaling is limited to the radius coordinate. The consequences are that, first, rotation can easily be determined by means of cross correlation, and second, the magnitude spectrum of the magnitude spectrum in polar coordinates is invariant with regard to cyclic shifts which actually represent the rotation of the original image.

Finally, a logarithmic transformation of the r-axis transforms the image scaling into a shift by $\ln(\alpha)$:

$$|F'(\rho,\Theta)| = \frac{1}{\alpha^2}\left| F\left(\rho-\ln(\alpha),\ \Theta+\beta\right)\right| \quad (5)$$

$$with\ \rho = \ln(r)$$

The image transformation into polar coordinates followed by a logarithmic transform of the r-axis is called a "log-polar" transformation. The results of these transformations indicate a simple way to determine the scaling differences of two images by just calculating a cross correlation function. It also becomes evident that by calculating the power spectrum of the log-polar transformed image a representation is obtained that is invariant with regard to the scale factor, too. The complete transformation uncouples translation, rotation and scale, and thus leads to a triple invariant image representation which lends itself to a very effective and fast algorithm for image registration as shown in figure 3. [1,2,3]

The procedure to register two images, based on the

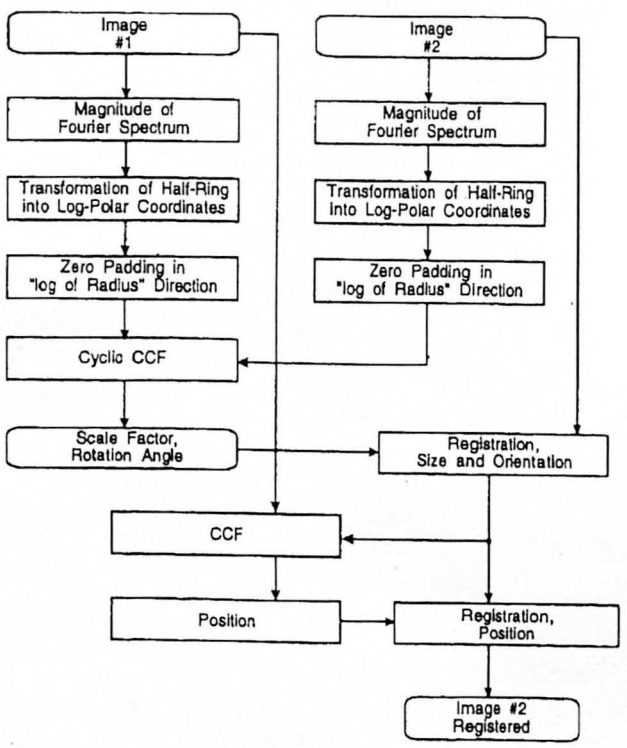

Fig. 3. Flow diagram for image registration based on triple invariant image description.

triple invariant image description works as follows. First, the magnitude of the Fourier spectrum of both images is determined. The transformation of a half-ring into log-polar coordinates is followed by expansion with zeros in the direction of the radius logarithm. The coordinates of the maximum of the cross correlation function determine the scaling factor and rotation angle necessary for image registration. One of the images is rotated and scaled accordingly. The correlation between the original image #1 and the registered image #2 now yields the differences in position. After an appropriate compensation of the translation the images are registered.

Reliability and precision of the procedure have been tested very successfully with different imaging modalities, including fundus photography, X-ray CT, nuclear medical images and ultrasound images. In addition to performing crossvalidations [3], test images were shifted, rotated, and scaled and the calculated transformation parameters were compared with the known manipulations. The errors basically corresponded to the computer precision. For a series of fundus images the identified errors could be neglected as they were smaller than one picture element for translation, smaller than 0.1° for rotation and smaller than 0.1% for the scaling factor. Even after superimposition of additional noise onto the images, the resulting errors were significantly smaller than those achieved by a human expert by means of interactive registration, which means a substantial improvement as compared to former methods of automatic image registration in medicine. At the same time, a drastical reduction was achieved for the computational amount required.

APPLICATIONS

Invariant image description has been proven as an extremely successful image processing technique in a number of clinical applications in nuclear medicine, ophthalmology, neurology, and cardiology. Several specific applications, representative for the broad range of diagnostic procedures where invariant image description is an important tool, will be discussed in the following: renal studies, diagnosis of retinitis pigmentosa, diagnosis of Alzheimer's disease, quantification of aortic stenosis, and the determination of stroke volume.

Dynamic Renal Studies

For functional control of the kidneys a series of images is taken with a gamma camera. In these images the concentration of a radio tracer is determined over a longer period of time, and by analysing the concentration curve, the renogram, the kidney function can be judged. Since it is often impossible to avoid movements of the patients during image acquisition, especially in the case of children, the kidneys move within the images accordingly, thus impeding the consistent counting of radio impulses within the chosen region of interest (ROI), supposedly the boundaries of the kidneys. In many cases the movements even mandate a repetition of the procedure. Through invariant image description and registration, which compensate for the motion artifacts, a repetition of the procedure can be avoided, thus reducing the stress for the patients and considerably lowering the costs of the renal studies [4].

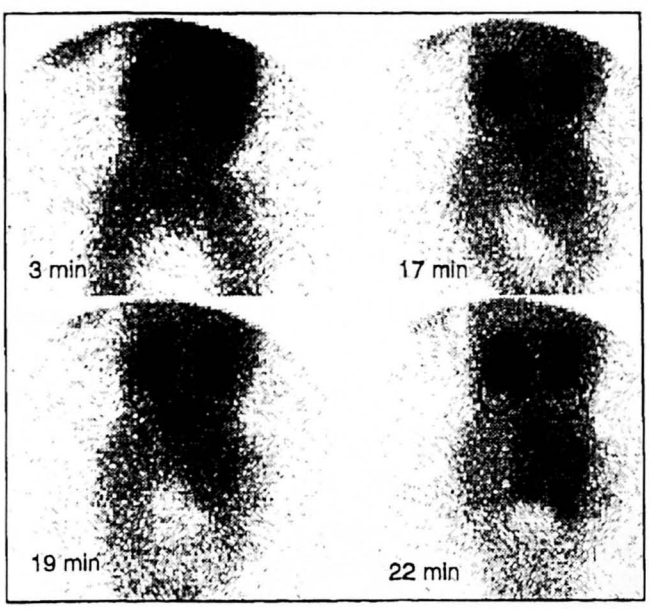

Fig. 4. Renal scintigraphic images with superimposed ROIs, showing the effect of patient motion. The ROIs have been selected in the first image of the shown sequence (3 min), and are applied to the following images without change of their position.

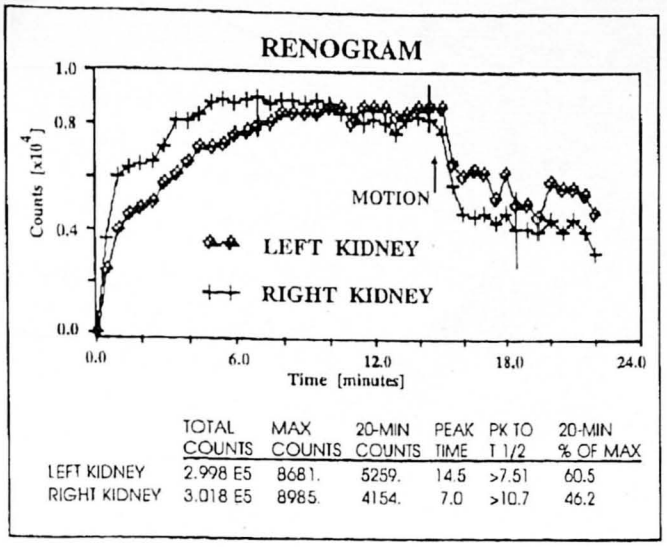

	TOTAL COUNTS	MAX COUNTS	20-MIN COUNTS	PEAK TIME	PK TO T 1/2	20-MIN % OF MAX
LEFT KIDNEY	2.998 E5	8681.	5259.	14.5	>7.51	60.5
RIGHT KIDNEY	3.018 E5	8985.	4154.	7.0	>10.7	46.2

Fig. 5. Erratic renogram, showing a substantial drop in counts as the effect of patient motion after the 15th minute, indicated by the arrow.

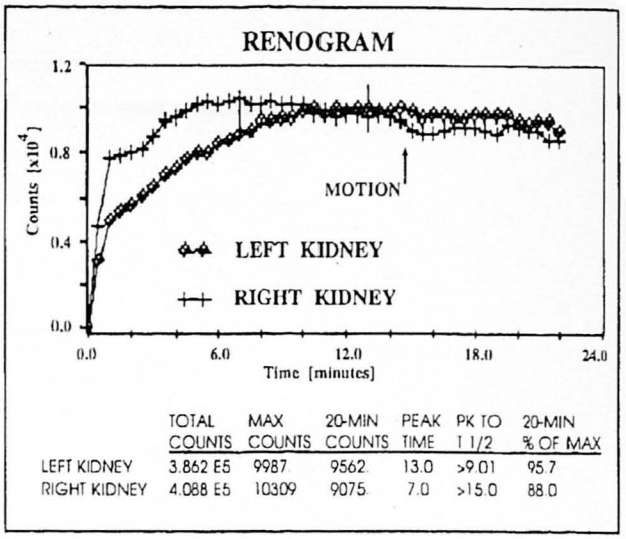

	TOTAL COUNTS	MAX COUNTS	20-MIN COUNTS	PEAK TIME	PK TO T 1/2	20-MIN % OF MAX
LEFT KIDNEY	3.862 E5	9987.	9562.	13.0	>9.01	95.7
RIGHT KIDNEY	4.088 E5	10309.	9075.	7.0	>15.0	88.0

Fig. 6. Corrected renogram, obtained from the same image study as in figure 5, but after compensation of patient motion. The renogram shows no more unphysiological decline at the time of the patient motion which is indicated by the arrow.

The problem is demonstrated in figures 4 and 5. After a patient movement slightly more than 15 minutes into the study, the outlined areas of interest do no longer completely cover the kidneys. Automated counting within the ROIs leads to a sudden, erroneous drop of the renogram. Redefining the ROIs after the motion occurs does not provide the necessary accuracy to eliminate the motion artifacts. Sequential registration of the whole series of images, on the other hand, completely compensates all translations and rotations and eliminates the influence of patient movements on the test as can be seen in figure 6. In the example shown here, the motion artifacts are obvious. In the case of small and slow movements, however, the motion artifacts can influence the measurement unnoticed if not prevented by proper image registration.

Investigation of Retinitis Pigmentosa

Another interesting application of invariant image description is found in ophthalmology for the diagnosis and long term surveillance of fundus diseases. A special project, conducted in cooperation with the Bascom Palmer Eye Institute in Miami, is the investigation of the origins of retinitis pigmentosa. Retinitis pigmentosa is a hereditary disease of the fundus and causes blindness in its progress. There is no cure yet.

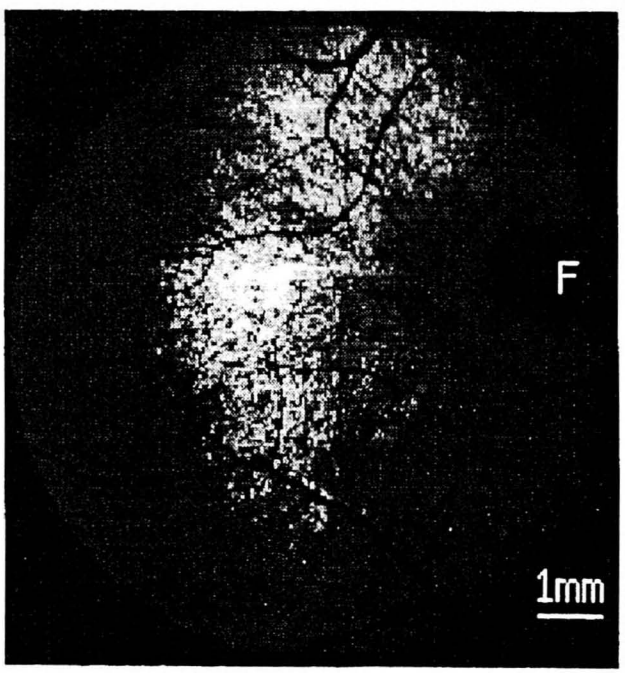

Fig. 7. Digitized fundus photograph of the right eye of an X-linked RP carrier with tapetal-like reflex; the darker region at the right is the Fovea (F), dark lines are retinal blood vessels, and the tapetal-like reflex shows as bright tiny reflections distributed throughout the fundus, especially left of (temporal to) the fovea. the calibration bar is approximately 1 mm, measured on the retinal surface.

Photographs of the fundus are taken for the diagnosis. A characteristic symptom of retinitis pigmentosa are golden-yellowish reflexes that seem to be radially oriented towards the fovea. In the enlargement the reflexes appear as blurred golden spots. The blurring is to a large extent caused by distortions during image acquisition. For the analysis of the reflexes an exact model of the imaging system has been determined, on the basis of which image reconstruction filtering cancels most of the noise and improves the sharpness of the reflexes. The reflexes are then isolated and analysed. Comparison of pictures taken over the course of time for the purpose of judging the development of the disease requires very accurate image registration which is performed based on the triple invariant image description. Even fundus images taken 23 years apart, exhibiting major differences in image quality, could be successfully registered as can be seen in figures 8 and 9. Surprisingly, there are only minor changes of the fundus over this long period of time.

It was the goal of the analysis of the reflexes to determine by structural analysis which of the cells are the cause for or the origin of the formation of the reflexes. For this purpose, a segmentation was performed on the reconstructed images, isolating the reflexes, and allowing their morphological analysis. The distributions of reflex size, shape, orientation, intensity and density were determined for both qualitative and quantitative analysis. Altogether, the results have lead to the hypothesis that the reflexes originate in the cones. Further studies have indeed confirmed that the first recognizable abnormalities appear in the photoreceptor system [2].

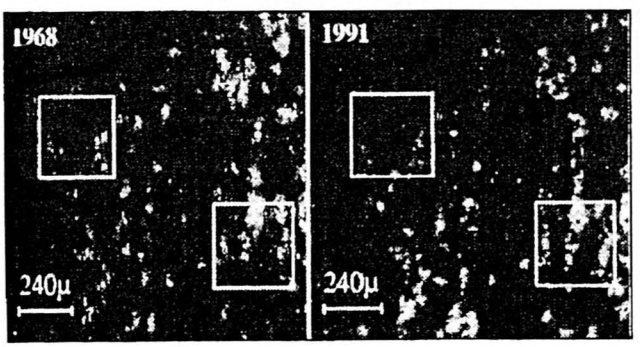

Fig. 8. Two fundus images of the same patient, taken 23 years apart. The images, showing a small area of the actual photographs, have been registered by invariant image description and then truncated to show the same region of the fundus. Except for the differences in image quality, mainly caused by the films used, little difference can be seen. The areas inside the marked squares are shown in figure 9 in a larger magnification to allow a more detailed comparison of the reflexes.

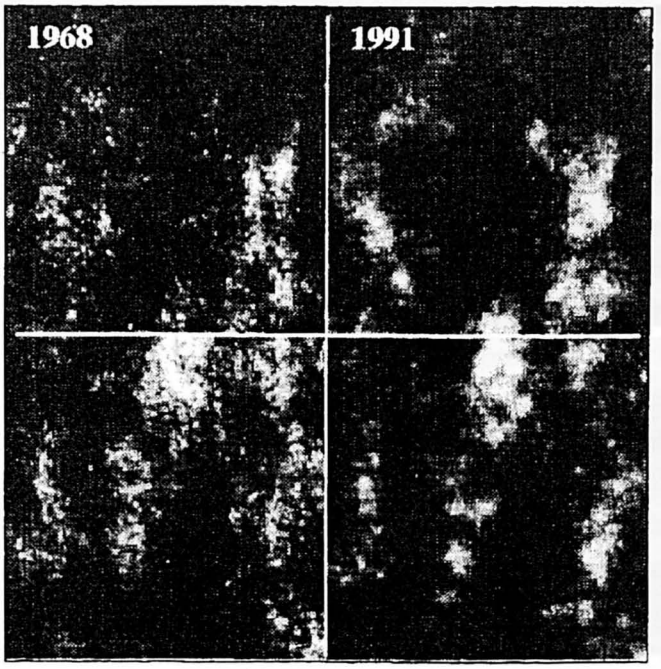

Fig. 9. Development of the tapetal-like reflexes in the right eye of an X-linked RP carrier. The pictures have been taken 23 years apart. No significant changes can be observed. The images show the fundus regions marked in figure 8. The size of the areas is 240×240 µm.

Diagnosis of Alzheimer's Disease

Reliable diagnosis of Alzheimer's disease, a major medical problem, can be achieved through the analysis of regional brain activity using neural networks. The values for regional brain activity are obtained from PET Scans which are segmented with the help of matching magnetic resonance images. Again, invariant image description is an extremely helpful tool for the necessary registration of PET and MRI scans.

A system for image based diagnosis of mental

diseases has to perform four different tasks:

- image registration and combination of the anatomic and metabolic information obtained by PET and MRI,
- a segmentation for the determination of activity in the different brain regions based on the higher resolution MRI,
- regional feature extraction within the PET image, and,
- data interpretation, i.e. diagnosis.

Data analysis is done by a back-propagation neural network. The output of the network shows either a yes/no decision or, if implemented using fuzzy logic, it indicates continuous probabilities for the decisions whether the patient suffers from Alzheimer's disease or not. The network has been trained by known cases. Different steps of anatomic "resolution" were tested, starting with the division of the brain into 67 small structures, then limiting the resolution to the activity patterns of the 25 lobules, and finally attempting a diagnosis on the basis of the eight lobi cerebri, four per hemisphere as shown in figure 11.

A comparison of results for the diagnosis of Alzheimer's disease as obtained by a human expert, discriminante analysis and neural network is shown in figure 12. The ROC curve or Relative Operating Char-

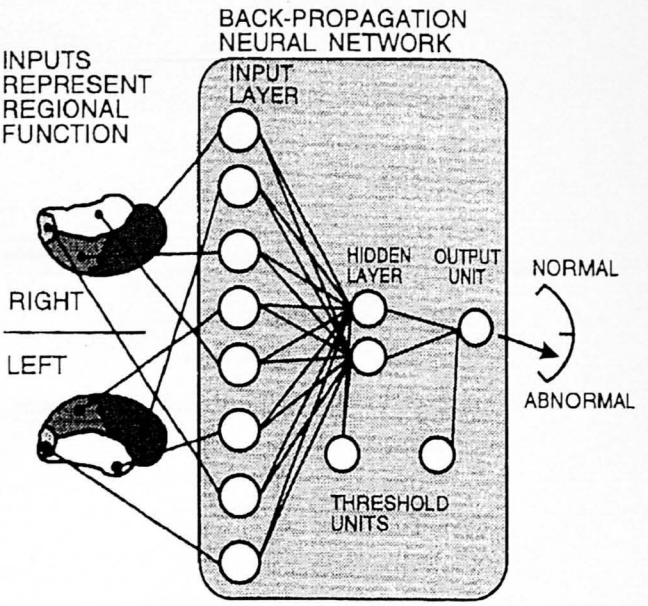

Fig. 11. Classification of mental disorders by a back-propagation neural network. The inputs are the regional rates of metabolic activity, the output is the probability for the presence of the disorder to be classified.

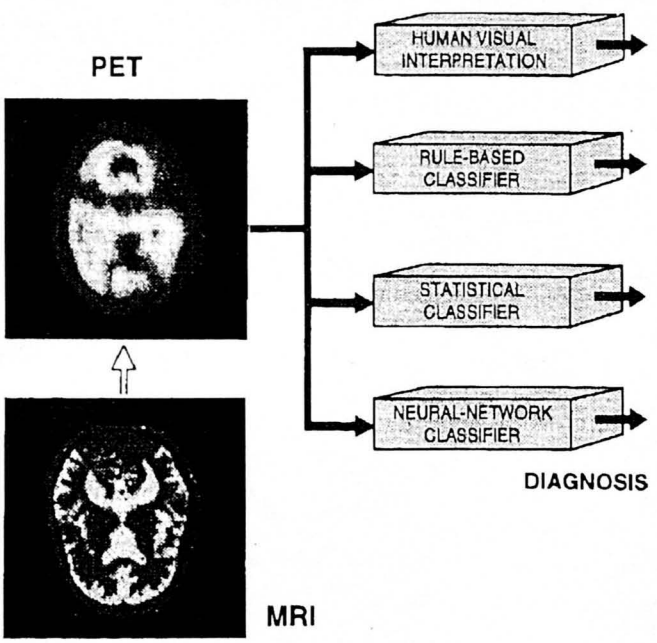

Fig. 10. Diagnosis of mental disorders based on PET imaging. MRI scans support the segmentation of the brain. Different methods for classification are tested.

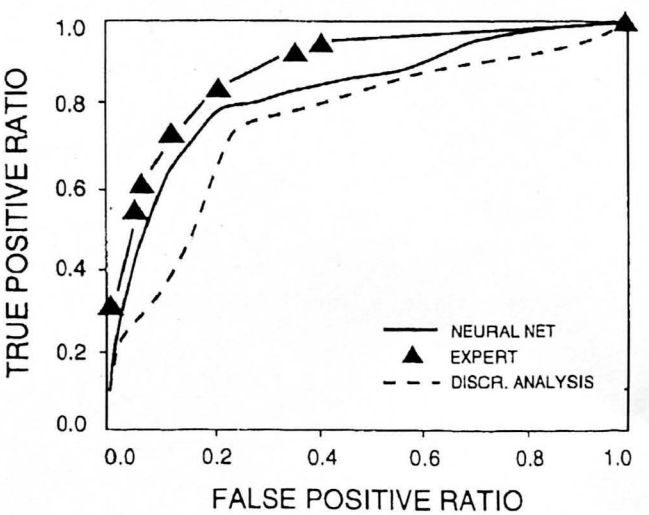

Fig. 12. ROC curves for the diagnosis of Alzheimer's disease based on PETTV images of the brain activity in the 25 lobules.

acteristics serve as a measure of efficiency. The area under the ROC, which indicates the probability of a right decision when a single case has to be decided by a clear yes or no, is the strongest indicator for the quality of the individual diagnostic technique. The human expert shows the best results, the worst were obtained by statistical analysis. It should be mentioned, however, that when comparing the performance of human expert and neural network, the human expert has a huge advantage because the validity of the neural network's decisions is judged by this expert, as a reliable verification of the diagnosis is only possible post mortem. By following up on the patient population used for this study, the ROC might over time actually shift in favor of the neural network. The profiles established by the neural network show the characteristic distributions of brain activity in the presence of the disease.

An interesting question is, whether the quality of the diagnosis is a function of image resolution, i.e. whether the huge costs of the latest PET systems with increased resolution can actually be justified from a diagnostic point of view. To investigate this issue, the ROCs of the two available systems, PETTV with a slice thickness of 15mm and Scanditronix with a slice thickness of 6mm, each for eight lobes and 25 regions, have been determined. An additional parameter for the performance was the kind of data standardization - absolute standardization versus standardization with regard to the activity value within the occipital brain lobe. As can be seen from the results shown in figure 14, the higher resolution system in fact improves the reliability of the diagnosis.

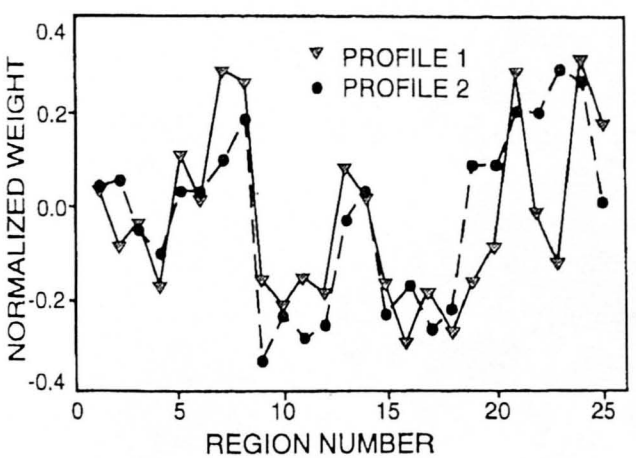

Fig. 13. Two characteristic patterns are obtained for the diagnosis of Alzheimer's disease by the back-propagation neural network with one hidden layer when fed with the functional activity in 25 brain lobules.

Quantification of Aortic Stenosis

Noninvasive assessment of valvular stenosis, valvular insufficiency, prosthetic valve function, congenital abnormalities, and to some extent, left ventricular function, can be achieved with the aid of Doppler echocardiography. The audio signal contains qualitative information about the characteristics of flow -laminar or turbulent- as well as quantitative information regarding the velocity distribution of blood flow. Using the Bernoulli equation, the information contained in the US signal permits to assess the severity of valvular stenosis. Some severe limitations of this technique lead to a further interesting application of invariant image description: the quantification of aortic stenosis.

The velocity of the blood flow entering the aorta is

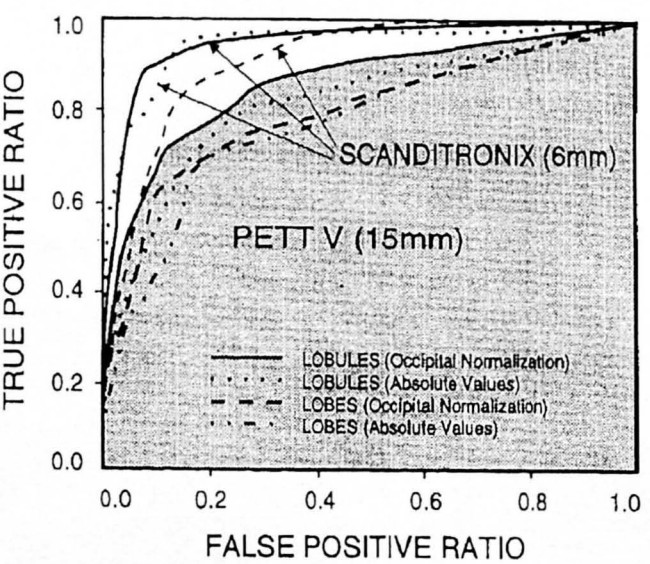

Fig. 14. Comparison of ROC curves for the PETTV and Scanditronix PET scanners. The higher resolution clearly allows superior reliability of diagnosis.

measured by Doppler US. According to the contraction of the heart and the opening characteristics of the aortic valve, the flow complexes exhibit a typical shape with a fast increase in flow velocity. In the healthy human the complexes have a rather constant shape. With an aortic valve stenosis the increase in blood flow velocity is distinctly reduced because of the incomplete opening of the aortic valve. The maximum of the blood flow velocity appears delayed as compared to a valve that opens completely.

Quantification of the stenosis is done mostly by determination of the gradient specifying the increase of blood flow velocity [7,8]. Figure 15 shows characteristic flow complexes for cases of mild, severe and critical stenosis. Precision and reliability of this procedure to quantify valvular stenosis remain uncertain, especially in elderly patients, particularly because of the frequent occurrence of arrhythmias, which cause significant variations in stroke volume and thus in signal amplitude and complex duration.

Accurate determination of the gradient is not easy because of the poorly defined, blurred outlines of the US signal. In principal, the gradient should be independent of stroke volume, i.e. the shape of the individual complexes should remain constant even in the presence of major variations of stroke volume. If this hypothesis can be proven, then it would be possible to develop a technique for the quantification of aortic stenosis that would lead to the same value, no matter which individual heart beat has been picked for the calculation. Invariant image description actually permits easy verification of this

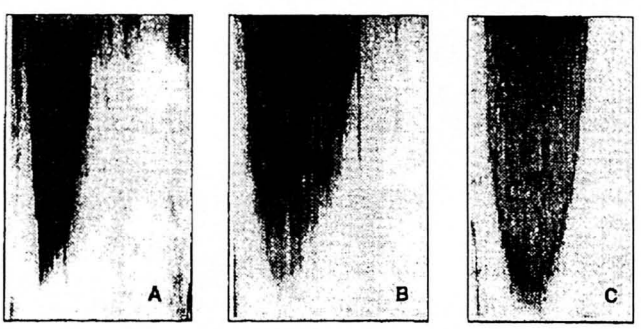

Fig. 15. Characteristic US Doppler signals for cases of mild (A), severe (B), and critical (C) aortic stenosis.

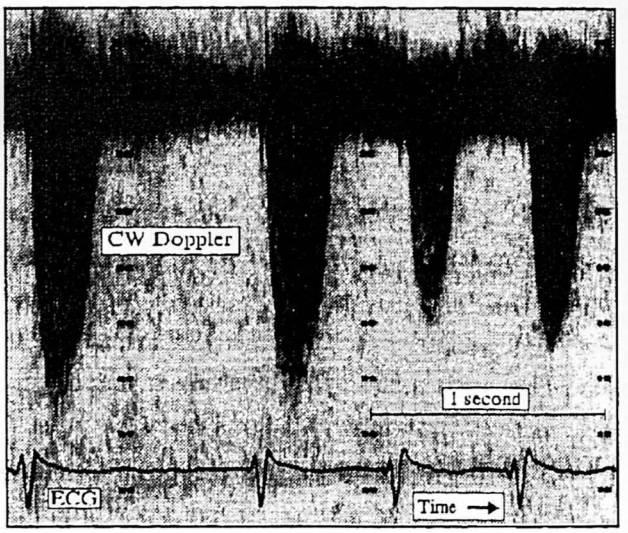

Fig. 16. Arrhythmia and the resulting variations in stroke volume as seen in the CW Doppler echocardiogram.

theory if the individual complexes are considered as a series of digital images and their correlation is examined after registration.

Rotation is not to be expected as a registration parameter in this application, instead the previously assumed uniform scaling factor has to be replaced by two independent factors for the horizontal and vertical image scale. Changes in stroke volume result from decreased flow velocity, diminishing the height of the ejection complex, and shortened ejection period, reducinging the width of the complex. In spite of ECG triggered image acquisition the start of the ejection complex is subject to time shifts because of the physiological variation of the pre-ejection period. This translation disappears in the magnitude spectrum of the image. Since there is no rotation, a transformation into polar coordinates is not helpful for the invariant image description, a double logarithmic transform is performed instead.

The double logarithmic transform converts both scaling factors a and b into an image translation. By calculating the power or magnitude spectrum a description of the US images is obtained that is invariant with regard to the scaling factors, i.e. amplitude and duration of the signal. Calculating the correlation between consecutive complexes exhibits their similarity and thus

answers the question whether the pattern remains constant in spite of variations of stroke volume.

$$\textit{Scaling:} \quad f(ax, by) \multimap \frac{1}{|ab|} F\left(\frac{u}{a}, \frac{v}{b}\right)$$

Log/LogTransform:

$$F'(u', v') = \frac{1}{|ab|} F(u'-\ln(a), v'-\ln(b))$$

$$\textit{with:} \quad u'=\ln(u), \quad v'=\ln(v) \qquad (6)$$

Results of the correlation analysis impressively confirm the intra-patient constancy of the pattern [8]. The correlation coefficients are well above 0.9 with only minimal standard deviation. As expected, the highest beat-to-beat fluctuations are recognizable for the signal amplitude, i.e. the maximum flow velocity during systole, with a standard deviation of up to 30%, whereas the ejection time changes considerably less, up to 10%.

These results indicate that diagnosis as well as quantification of the aortic stenosis should indeed be independent of the choice of the single complex analysed if the appropriate criteria are applied. Furthermore it means that for the actual quantification the appropriate parameter can be derived from the scale invariant representation of the images. In a first clinical study several standard patterns, representative for various degrees of aortic stenosis have been developed. Correlating the actual Doppler signal and the standard patterns - both independent of signal duration or amplitude respectively - appears to enable safe classification and thus quantification of aortic stenosis.

Determination of Stroke Volume

With the development of ultrafast X-ray CT scanners (Imatron), it has become possible to perform high-resolution dynamic cardiac studies. In addition to the assessment of many other medically interesting parameters, the noninvasive determination of stroke volume with unprecedented reliability and precision is an application of special interest - not only for clinical diagnostics but also as a valuable tool for the validation of other, less expensive techniques for stroke volume determination, such as impedance cardiography.

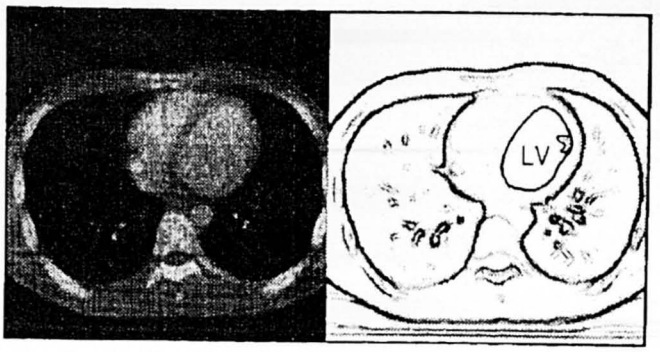

Fig. 17. A cross sectional view through the heart, as it is obtained with the Imatron ultrafast CT scanner, is shown in the left panel. The right panel shows the image after contrast enhancement and contour detection for the left ventricle.

In order to determine the stroke volume, ten to twelve sections of the heart are obtained in a short axis view at the end of the diastole and the end of the systole. A 3-d reconstruction renders the left ventricular volume. The difference in end diastolic and end systolic volumes of the left ventricle yields the stroke volume. Since the images are not all obtained at the same time, but rather distributed over several heart beats, they have to be registered with regard to the heart before the 3-d image can be reconstructed. After registration, the endocardium is detected and the stroke volume is determined. Again, invariant image description is the tool of choice for the image registration.

In a validation study, stroke volumes obtained with the ultrafast CT scanner and with impedance cardiography have been compared. Impedance cardiography (ICG) measures the thoracic impedance as well as its changes related to the pulsating blood flow in order to determine cardiac time intervals and stroke volume [9].

The stroke volumes obtained by ICG and CT show excellent correlation of r=0.935 for resting condition of healthy subjects, as shown in figure 18. In an experiment where a change of stroke volume has been induced by the infusion of dobutamine, a very strong correlation of stroke volume changes (r=0.95) was seen as well. These results prove excellent reliability and precision for both the ICG system and the image registration based on invariant image description.

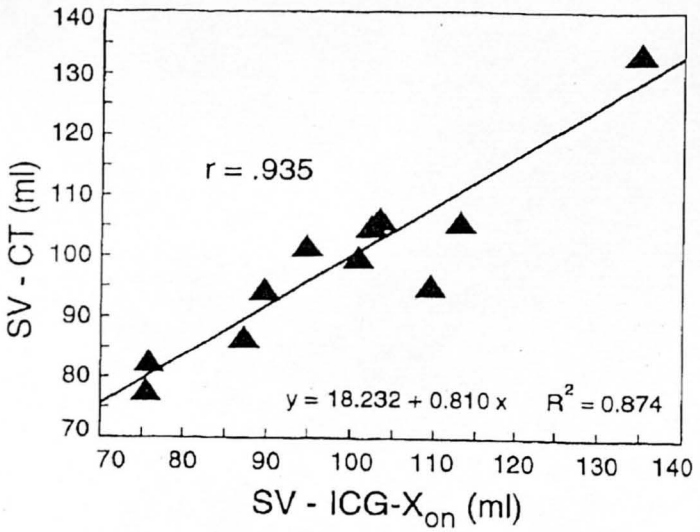

Fig. 18. Comparison of stroke volumes calculated from CT scans and through impedance cardiography (inspiratory breath-hold).

SUMMARY

In summary, invariant image description has proven to be an extremely successful tool for medical image processing and has already contributed significantly to the improvement of clinical diagnostics. The technique has been widely acknowledged as being superior to other methods of image registration. Further applications, not limited to medical diagnostics, are to be expected.

REFERENCES

1. Apicella A, JS Kippenhan, Nagel JH: Fast multimodality image matching. Medical Imaging III, SPIE 1989; 1092: 252-263.
2. Cidecyan AV, Jacobsen SG, Kemp CM, Knighton RW, Nagel JH: Registration of high resolution images of the retina. Medical Imaging VI, SPIE 1992; 1652: 310-322.
3. Nagel JH, Cideciyan AV: Digital analysis of high resolution fundus images. Biomedical Engineering Appl Basis Comm 1992; 4: 645-682.
4. Georgiou MF, Nagel JH, Cideciyan AV, Sfakianakis GN: Compensation for patient motion in nuclear medicine renal studies by fast correlation image registration. Proceedings of the Annual International Conference of the IEEE/EMBS 1993; 106-107.
5. Kippenhan JS, Barker WW, Pascal S, Nagel J, Duara R: Evaluation of a Neural-Network Classifier for PET scans of normal and Alzheimer's disease subjects. J Nucl Med 1992; 33: 1459-1467.
6. Kippenhan JS, Barker W, Nagel J, Grady C, Duara R: Neural-Network classification of normal and Alzheimer's disease subjects using high-resolution and low-resolution PET cameras. J Nucl Med 1994; 35: 7-15.
7. Agatston AS, Chengot M, Rao A, Hildner F, Samet P: Doppler diagnosis of valvular aortic stenosis in patients over 60 years of age. Am J Cardiol 1985; 56:106-109.
8. Zahn T, Nagel JH, Agatston A: Quantification of aortic stenosis based on the morphologic structure of Doppler ultrasound signals using image processing techniques. Abstracts of the World Congress on Medical Physics and Biomedical Engineering, 1994.
9. Nagel JH, Shyu LY, Reddy SP, Hurwitz BE, McCabe PM, Schneiderman N: New signal processing techniques for improved precision of noninvasive impedance cardiography. Annals of Biomedical Engineering 1989; 17: 517-534.